ingegneria sismica
International Journal of Earthquake Engineering
Anno XLIII - Num. 1 - 2026

The Path of Digital Protection and Innovative Development of Red Cultural Resources Supported by Intelligent Information

Dan Wu[1,*]

[1] Humanities and Foreign Languages Department, Xi'an Aeronautical University, Xi'an, Shaanxi, 710077, China

SUMMARY: *In this paper, deep learning, 3D scene modeling, and resource sharing platform are used to solve the protection and inheritance challenges faced by red cultural resources due to age erosion. Firstly, a triple-domain transformation network based on variational autoencoder (VAE) is introduced to realize historical photo restoration. The point cloud simplification algorithm with limited normal precision is adopted in the 3D reconstruction, and the point cloud data is woven into a 3D model by the partitioning algorithm. Finally, based on the resource management strategy of "distributed storage, centralized management", the physical resources are distributed and the key index information is centrally managed to achieve standardized resource sharing. The photo restoration model based on VAE has PSNR=38.98 and SSIM=0.912 in the red cultural history RealPhoto dataset, which is 6.24% and 6.17% higher than the second place TDT model. In the subjective evaluation, more than 82.96% of users rated the VAE restoration effect as the first place. For 3D reconstruction, the partitioning algorithm leads the average performance on the ShapeNet dataset across the board, with a CD value and F1 score of 0.32 and 83.91, respectively, which are both better than the point-by-point insertion method and the triangular mesh growth method. In the resource sharing efficiency test, even if the amount of resources increases to 5000, the uploading efficiency of the hybrid model in this paper is still stabilized at a high level of 93.4%, and in the anti-jamming test, its network request acceptance rate is kept at 100%.*

KEYWORDS: *red resources; variational autoencoder; 3D scene modeling; historical photo restoration; partition algorithm; resource sharing model*

1 Introduction

With the progress of science and technology, China has ushered in the Internet era, online shopping, online grocery shopping, online office and so on have been the norm in life, the Internet has been closely related to people's lives. The Internet also plays an important role in politics, culture and education, and it is no exception for the protection and innovative development of red cultural resources [1]. Since its creation, red culture has enriched the spiritual world of Chinese people, improved the quality of Chinese people, and cultivated the sentiment of Chinese people. China's red culture is hard-won and must learn to inherit and carry forward, learn to innovate and protect. However, with the continuous development and change of science and technology, the digitization of cultural protection supported by intelligent information is becoming more and more popular and has shown great advantages [2, 3]. Relative to other protection measures, the digital protection and innovation of red cultural

*344575804@qq.com
https://doi.org/10.65102/is2026011
Published: 30 April, 2026

resources not only keeps pace with the times, but also improves the means of protection, makes the protection of red culture more convenient, and promotes the dissemination and development of red cultural resources [4, 5].

Digital protection refers to the digitization of physical red culture, and preservation, dissemination and utilization through the corresponding technical means, digital protection can effectively protect the integrity and safety of cultural relics, so that the red cultural resources can be preserved for a long time, and at the same time, it is also convenient for the public to learn and understand the cultural relics [6-8]. In terms of digital protection and innovative development of red cultural resources, there are mainly intelligent technology, electronic storage, regular inspection and other paths. Through digital technology and intelligent technology, three-dimensional scanning, virtual reconstruction and other operations can be carried out on red cultural resources, enabling the digital preservation of cultural relics [9-11]. At the same time, after digitizing the cultural relics, the three-dimensional display of the cultural relics can also be realized through virtual reality technology and other ways to improve the public's visiting experience. And electronic storage is one of the important means of digital preservation [12-14]. By digitizing cultural relics and storing them in electronic devices, the safety and sustainability of cultural relics can be better ensured. At the same time, electronic storage also facilitates public learning and understanding. Another important part of digital protection is regular inspection, which regularly checks the safety and integrity of digital storage devices to ensure that cultural relics can be preserved for a long time and that problems such as damage and loss of cultural relics are detected and dealt with in a timely manner [15-17].

With the support of intelligent information, the digital protection and innovative development of red cultural resources show diverse characteristics. For example, literature [18], based on the protection and innovative development of red culture, utilizes a distributed machine learning system implemented in a system architecture of parameter servers, revealing that the development of red cultural resources is in line with the expected assumptions under the intelligent simulation of the machine learning system. Literature [19] describes a path for the protection and innovative development of red cultural resources, i.e., digital storage, and through display and dissemination, which helps to enhance the audience group and facilitates red cultural education. Literature [20] designed a series of red culture and creative products based on Guangxi red culture, using immersive interactive experience and augmented reality technology, combining digital applications with red culture, which contributes to the protection and innovative development of red cultural resources and enhances the user experience. Literature [21], based on the theory of landscape genes, explains the necessity of integrating landscape genes into the digital protection of red culture, and discusses the technical path of digital presentation of red culture, exploring its digital presentation methods from digital modeling, digital platform construction and other aspects. Literature [22] explored the innovative design mode of red culture and creative product design, extracted the design elements of red culture based on computer digital technology, and presented them to consumers in a perceptible form through innovative design. Literature [23] aims to discuss the balanced protection and display of tourism development and red cultural resources in the digital era, revealing the digital protection mode of red cultural resources, open-air museums, enhancement of digital experience, and online communication. Literature [24] explored the digitization and preservation of red music cultural heritage as well as the exploration of dance narratives, and based on the literature review emphasized the role of digital technology in the preservation of red music artifacts, including high-resolution audio recording, 3D scanning, and digital archiving systems. Literature [25] analyzed the application of digital media technology in the

creation of red animation based on the development of digital media technology through the cooperation of universities, governments and enterprises, showing that digital media technology brings positive effects to red animation, effectively transmitting and promoting red culture.

In addition, literature [26] outlines the application of virtual reality technology in red culture exhibition halls, realizing immersive visits, and with its simulation and reproduction of the actual scene, enabling the public to immerse themselves in the scene and personally feel the revolutionary enthusiasm of red culture, and promoting the innovation and development of red culture. Literature [27] discusses the use of digital technology to empower the innovative transformation of red cultural resources, aiming to enhance the educational value and social influence of red cultural resources, provide strategic guidance for its future digital transformation, and promote its innovative development. Literature [28] investigates the role of augmented reality technology in promoting the cultural and creative transformation of traditional cultural resources, based on application examples showing that augmented reality technology promotes the development of cultural and creative industries of traditional culture and enables its better reconstruction. Literature [29] discusses the application of digital technology in red culture and tourism fusion attractions, aiming to provide practical guidance for the digital application in red and cultural tourism fusion venues, and suggests that it focuses on the selection and optimization of digital technology in order to enhance the visitor experience and sense of cultural identity. Literature [30] describes the combination of emotional design theory and red culture to enhance user experience satisfaction, so as to provide new ideas for the effective inheritance and promotion of red culture in the new era. Literature [31] explores the construction and application of the digital protection and dissemination system of red cultural resources based on the Internet of Things and big data technology, which provides a scientific method and feasible path for the digital transformation of red cultural heritage.

With the rapid development of artificial intelligence and three-dimensional digitization, numerous effective means of digital conservation have emerged. The study realizes the restoration and reconstruction of red cultural resources based on the simplification of its potential spatial domain and limited normal precision. Firstly, for 2D historical photos, a restoration technique based on variational autoencoder VAE is proposed. The degradation types of the photos are identified - global noise, fading or local scratches and holes. Learning how to translate the broken image back to its original form in the hidden space dimension through triple-domain transformation. For the 3D scene of the site, the first step is to use a simplified algorithm with limited normal precision to process the point cloud data obtained through laser scanning. The simplification of the point cloud is achieved by limiting the surface normal accuracy. Subsequently, the partition algorithm, a triangular mesh weaving technique, is introduced to mesh the point cloud data of millions of sites and finally stitch them together into a realistic and complete three-dimensional three-dimensional model. Finally, a set of “distributed storage, centralized management” red culture resource management strategy is proposed. Specific resources are distributed and stored in various places, while their key metadata are centralized and managed on a unified platform. It is convenient to find the precise location and detailed information of the data quickly in the search. Then, from the standardized production of resources, registration into the database, to the final release and use, to ensure the efficient sharing and utilization of digital assets.

2 Technological integration and management strategy for digital preservation of red cultural resources

2.1 Variational Self-Encoder Based Restoration of Historical Photos

2.1.1 Core ideas

Degradation of real photographs is a composite of multiple degradations, with not only spatially homogeneous unstructured defects: film noise, blurring, and fading; but also structured defects: holes, scratches, and speckles. Therefore, different repair strategies should be adopted for different types of defects: unstructured defects should be repaired using nearby pixels, and structured defects should be repaired using global image context information.

To address the above problems, this paper uses a triple-domain transformation network to convert the historical photo restoration problem into an image translation problem. Firstly, the clear and complete clean image and the degraded old photo are regarded as two domains, and then another image domain composed of artificially degraded synthetic photos is added, and then they are encoded into the corresponding hermitian space respectively by a variational autoencoder, and finally the mapping between the learned hermitian spaces completes the translation of the images, so as to achieve the purpose of historical photo restoration.

Figure 1 is a depiction of the triple domain transformation: R is the real historical photo domain, X is the artificially degraded synthesized photo domain, and Y is the unartificially degraded clean photo domain from the synthesized photo data. The images of the three domains are denoted by $r \in R$, $x \in X$, and $y \in Y$, respectively; x is the image artificially degraded from y, so x and y exist in pairs through data synthesis, and r is the real historical photo image. Since x and r are not pairwise images and are not suitable for supervised learning, the mapping from real historical photo $\{r\}_{i=1}^{N}$ to clean image $\{y\}_{i=1}^{N}$ is difficult, and the image transformation process will be divided into two stages next: firstly, the images in the three domain spaces R, X, Y will be mapped to the corresponding images by the encoders E_R, E_X, E_Y mapped to the corresponding hidden spaces $E_R : R \to Z_R$, $E_X : X \to Z_X$, and $E_Y : Y \to Z_Y$. Since both the synthesized pictures in the X domain and the real historical photos in the R domain are obtained by degradation, there will be some visual similarity and the distributions of the two will overlap to some extent, so we try to align their potential spaces to the shared domain, i.e., map them to the same hermitian space, by adding constraints, which results in $Z_R \approx Z_X$. The so-called aligned potential space is the dashed region in Fig. 1, in which all the features of the corrupted images in X and R will be encoded.

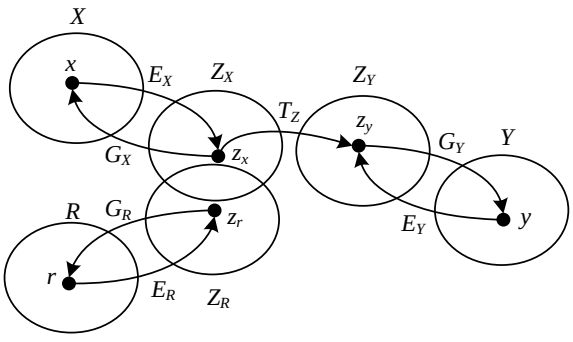

Figure 1: Three-domain transformation description

The second stage utilizes the synthetic data to perform the hidden space mapping $T_X : Z_X \to Z_Y$ on $\{x, y\}_{i=1}^{N}$ to learn the translation from the potential space of the artificially degraded synthetic photo to the potential space of the real image. After learning the translation transformation of the hidden space, the real historical photos can also be used to complete the image restoration by learning the translation of the potential space. The specific restoration is shown in Equation (1):

$$r_{R\to Y} = G_Y \circ T_Z \circ E_R(r) \tag{1}$$

where G is the generator, T is the mapping network, and E is the encoder.

2.1.2 Alignment of hidden spaces

The key point of the aligned potential space domain algorithm is to map the real historical photos and the synthetic degraded images into the same hidden space, so the variational autoencoder is proposed for compact coding, and then the domain gap of the image is further analyzed using generative adversarial network, and the basic network results are shown in Fig. 2.

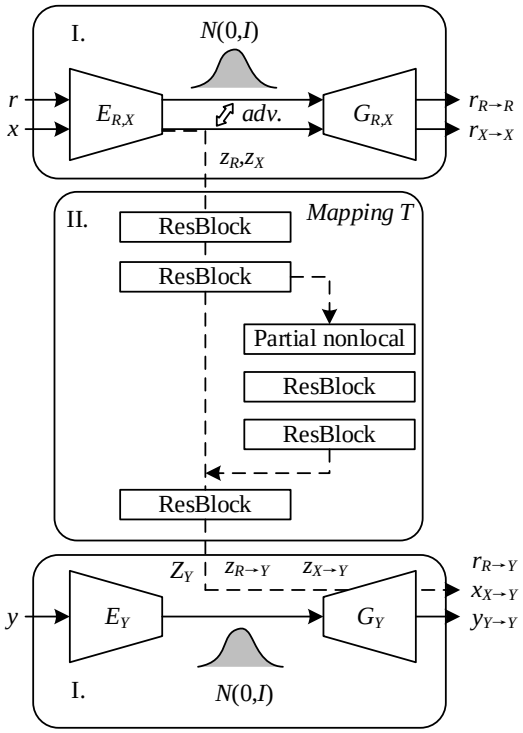

Figure 2: Basic network structure

Part I is to train the variational autoencoder VAE_1 shared by real historical photographs $\{r\}$ and artificially synthesized degraded historical photographs $\{x\}$, who encodes the image $\{r\}$ and the image $\{x\}$ into the latent space Z_R and Z_X through the encoder $E_{R,X}$, and lets the latent encodings all conform to a Gaussian distribution, and then perform random sampling and use generator $G_{R,X}$ to let the sampled data conforming to Gaussian distribution

for image reconstruction. When the input target is $\{r\}$, its objective function expression is shown in (2):

$$\begin{aligned} L_{VAE_1}(r) &= KL\left(E_{R,X}(z_r|\ r)\,\|\,N(0,I)\right) \\ &+\alpha E_{z_r\sim E_{R,X}(z_r|\ r)}\left[\left\|G_{R,X}(r_{R\to R}|\ z_r)-r\right\|_1\right] \\ &+L_{VAE_1,GAN}(r) \end{aligned} \tag{2}$$

In equation (2) $z_r \in Z_R$ is the potential encoding of the image $\{r\}$ generated by the encoder $E_{R,X}$, and $r_{R\to R}$ is the output of the image $\{r\}$ after encoding by the encoder and decoding by the decoder.

The first term of the objective function is the KL scatter, which is mainly used to constrain the distribution of the potential encoding, hoping that the encoding z_r produced by $\{r\}$ after the encoder $E_{R,X}$ is as similar as possible to the Gaussian distribution; the second term denotes the L_1 loss between the result recovered from VAE_1 encoding and the input data r, which is aimed at enhancing input The third term introduces LSGANloss, which is the generator's loss to prevent the VAE-generated results from being too smooth. Similarly, when the input target object of VAE_1 is x, the operation principle is exactly the same, because . The loss function $L_{VAE_1}(x)$ has the same form as $L_{VAE_1}(r)$ above.

Part I is another variational autoencoder VAE_2 to be trained, which is mainly used for clean images, and its objective function is defined in a similar structure as the objective function of r.

Since the image $\{r\}$ and the image $\{x\}$ share a common VAE, which makes the potential space of the two very close to each other, in order to bring the feature gap of the hidden space Z_R and Z_X closer, the adversarial network is chosen to check the remaining potential space, so the discriminator $D_{R,X}$ is trained to distinguish between the two potential encodings, and the corresponding loss function is defined as shown in Eq. (3) is shown:

$$\begin{aligned} L^{latent}_{VAE_1,GAN}(r,x) &= E_{x\sim X}\left[D_{R,X}\left(E_{R,X}(X)\right)^2\right] \\ &+E_{r\sim R}\left[1-D_{R,X}\left(E_{R,X}(X)\right)^2\right] \end{aligned} \tag{3}$$

The encoder of VAE_1 tries to trick the discriminator with a paradoxical loss to ensure that R and X are mapped to the same space, and combining this with the potential antagonistic loss, it can be shown that the total loss function of VAE_1 is designed as Equation (4):

$$L_{VAE_1} = \min_{E_{R,X},G_{R,X}} \max_{D_{R,X}} L_{VAE_1}(r) + L_{VAE_1}(x) + L^{latent}_{VAE_1,GAN}(r,x) \tag{4}$$

2.1.3 Repair Mappings in Hidden Spaces

The second stage of image transformation is to carry out the mapping in the hidden space, which mainly utilizes the synthetic data for $\{x,y\}_{i=1}^N$ to train a mapping network from the hidden

space Z_X to Z_Y, and then the image restoration is accomplished by the mapping network. The reason for choosing image restoration in the hidden space is that $Z_X \to Z_Y$ is easier and the mapping relationship between them will be simpler to learn, as long as R and X are aligned in the same hidden space, then the mapping from Z_X to Z_Y can be generalized to Z_R to Z_Y, and R can be restored; and secondly, it is better to build the mapping in a low-dimensional hidden space it is much easier to establish the mapping than in the high dimensional hidden space. In this stage, the main focus is to train the mapping network T between potential spaces based on the fixed trained VAE model. Here assume that the final outputs of r, x, y are $r_{R\to Y}$, $x_{X\to Y}$, $y_{Y\to Y}$, then the loss function $L_T(x, y)$ of the mapping network T can be obtained as defined in Eq. (5):

$$L_T(x,y) = \lambda_1 L_{T,l_1} + L_{T,\mathrm{GAN}} + \lambda_2 L_{FM} \tag{5}$$

The first term in the above equation is the L1 loss, which aims to make Z_X map to Z_Y with the expression:

$$L_{T,l_1} = E\left\| T(z_x) - z_y \right\|_1 \tag{6}$$

The second term in Eq. is the LSGANloss, in order to ensure that the output result of $x_{X\to Y}$ is more realistic, and the third term in Eq. is the perceptual loss function commonly used in VGG, which compares the difference between the true-false sample pairs in the middle layer of the discriminator and the middle layer of the VGG in order to stabilize the training of the GAN, in which the expression of L_{FM} is shown in (7):

$$\begin{aligned} L_{FM} = {} & E\left[\sum_i \frac{1}{n^i_{D_T}} \left\| \phi^i_{D_T}(x_{X\to Y}) - \phi^i_{D_T}(y_{Y\to Y}) \right\|_1 \right] \\ & + E\left[\sum_i \frac{1}{n^i_{VGG}} \left\| \phi^i_{VGG}(x_{X\to Y}) - \phi^i_{VGG}(y_{Y\to Y}) \right\|_1 \right] \end{aligned} \tag{7}$$

2.2 Reconstruction of the 3D scene model of the site

The digital protection of red cultural resources not only involves the above two-dimensional image recovery, but also requires three-dimensional digital reconstruction of cultural sites. In this regard, this section turns to the three-dimensional scene model reconstruction of the site, and realizes the generation of high-precision three-dimensional model through the point cloud simplification and meshing technology to provide support for the three-dimensional display and protection of red cultural resources.

2.2.1 Simplified algorithm for limiting normal accuracy

The simplification algorithm for large-scale point cloud data used in this paper is limited normal precision. The algorithm realizes the simplification of the point cloud by limiting the surface normal precision, and its main idea is: take the perpendicular distance from the measurement point to the corresponding least-squares fitting plane d_i as the approximate normal error

caused by deleting the point, and if d_i is smaller than the specified value of the normal precision, then the measurement point will be deleted.

$$d_i = \left|(x_i - O_i)\prod n_i\right| \tag{8}$$

The main steps of the algorithm are:
(1) Initialize the algorithm such that
Critical Accuracy = pre-specified normal accuracy

$$Canceled[i] = FALSE\,(i = 1, \cdots, N)$$

(2) For a certain measurement point x_i, if $Canceled[i] = TRUE$, check the next point; otherwise, calculate the approximate normal error d_i of x_i based on Eqn. (8), and if $d_i < CriticalAccuracy$, set it $Canceled[index] = TRUE$.

(3) Repeat (2) for all points in the whole point set.

(4) Delete all $Canceled[index] = TRUE$ points in the point set, and the simplification ends.

How to calculate the normal error caused by deleting a point is the key to realize the algorithm. To this end, the approximate tangent plane P_i of the surface M at the point x_i is constructed according to each measurement point x_i and its $k-$ nearest neighbor $Nbhd(x_i)$, and the normal accuracy is shown schematically in Fig. 3.

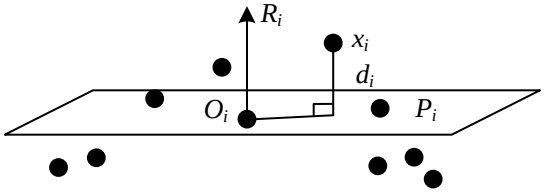

Figure 3: Normal accuracy illustration

P_i is the least squares fitting plane of the nearest neighbor $Nbhd(x_i)$ of the measurement point x_i, denoted by the form center O_i of $Nbhd(x_i)$ and the unit normal vector n_i.

$$O_i = \frac{1}{k}\sum_{p \in Nbhd(x_i)} p \tag{9}$$

The unit normal vector n_i can be determined by principal element analysis. First, the covariance matrix of $Nbhd(x_i)$, which is a 3 × 3 semi-positive definite matrix, is computed:

$$CV = \sum_{y_i \in Nbhd(x_i)} (y_i - O_i) \otimes (y_i - O_i) \tag{10}$$

where $\otimes$ is the sign of the outer product of vectors.

Let the 3 eigenvectors of CV be $\vec{v}_i^1, \vec{v}_i^2, \vec{v}_i^3$, and the corresponding 3 eigenvalues be $\lambda_i^1, \lambda_i^2, \lambda_i^3$, respectively.

If

$$\lambda_i^1 \le \lambda_i^2 \le \lambda_i^3 \tag{11}$$

Then

$$\left|n_i\right| = \left|\overrightarrow{v_i^3}\right| \tag{12}$$

For the red cultural heritage sites and such ancient buildings with complex geometric shapes, the simplified processing of their point clouds is more special, which requires fewer points to be distributed in the area of smaller curvature of the surface and more points to be retained in the area of larger curvature of the surface. Therefore, for the processing of point cloud data of this kind of buildings and precious affiliated cultural relics, the simplification method based on the limited normal accuracy should be adopted in order to preserve the point cloud data of the detailed features of the ancient buildings in a more complete way.

2.2.2 Reconstruction Method - Partitioning Algorithm

Because the topological relationship between three-dimensional scattered data points, i.e., point clouds, is very complex, the projection domain triangulation technique is mainly used at present to transform the dissection problem in three-dimensional space into two-dimensional space first, and then return to three-dimensional space after completing the triangulation. In this paper, we mainly adopt the partition algorithm in Delaunay triangulation to realize large-scale point cloud meshing.

The partitioning algorithm adopts a recursive partitioning strategy, which first divides the set of points to be small enough so that it is easy to generate the triangular mesh, and then merges the triangular mesh in the subset step by step from the bottom up and finally generates the complete triangular mesh. The basic steps of the algorithm are

(1) First arrange the point set V in ascending order based on (x, y) coordinate values, and then recursively execute steps (2)-(6);

(2) Divide the point set V into two approximately equal subsets VL and VR

(3) Generate sub-triangular nets in the subsets and;

(4) Local optimization of the generated triangular mesh into a Delaunay triangular mesh;

(5) Compute the bottom and top lines connecting the two convex hulls in the subsets VL and VR;

(6) Merge the two sub-triangular nets in VL and VR from the bottom line to the top line.

2.3 Management of red cultural resources

Based on the above two-dimensional or three-dimensional resource restoration of red resources, this section introduces the red cultural resource management strategy with the goal of realizing standardized resource integration and utilization, and proposes the mode of “distributed storage and centralized management” to ensure that the restored red resources, such as historical photographs and reconstructed three-dimensional models, can be efficiently stored, retrieved and published.

2.3.1 “Distribute storage, centralize management” resource management strategy

This paper combines centralized and distributed storage methods to form a “distributed storage, centralized management” storage method, so that resource management to achieve better results.

The low-granularity resources are distributed and stored in each management system, and the related information of resource packages is stored centrally and managed uniformly. The model is shown in Figure 4.

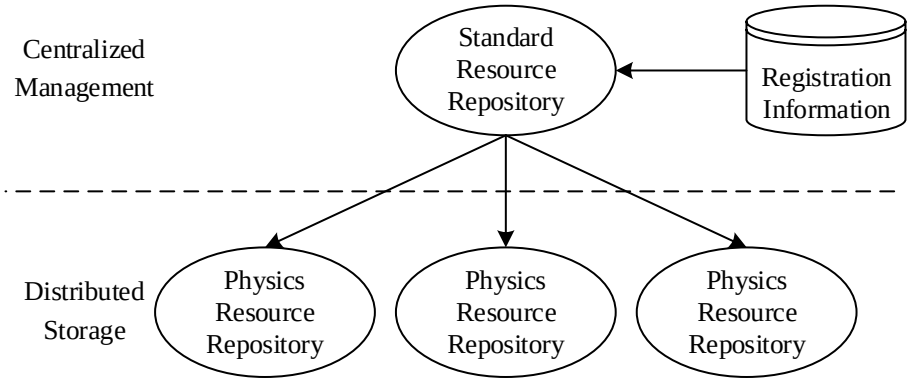

Figure 4: "Dispersed storage, centralized management" model

The hierarchical management model of learning resources is shown in Figure 5. The management model of learning resources is divided into three layers:

(1) Resource creation layer. Users develop standardized resources according to standardized specifications or resource creation software, complete resource creation, and register through the resource registration interface;

(2) Resource storage layer. Provide resource registration interface, content standardization and legality audit of uploaded resources, store resources after passing the audit, and store resource metadata information;

(3) Resource publishing layer. Successfully registered resources can be published on the Web platform for users to retrieve and access.

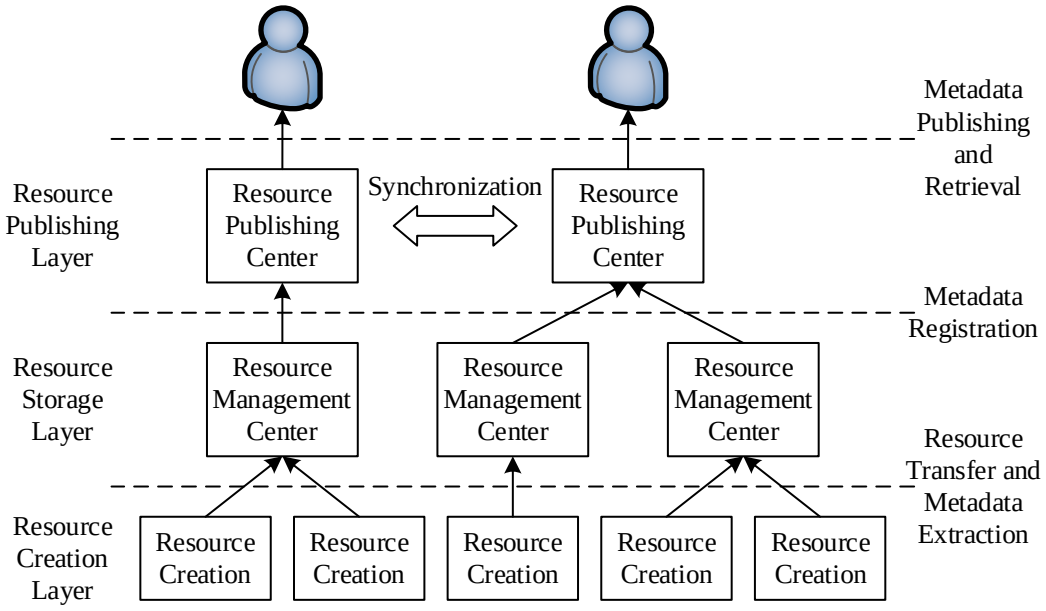

Figure 5: The hierarchical management model of learning resources

Combining the “distributed storage, centralized management” model and the hierarchical management model of learning resources, the resource management process of the platform is derived. The resource management process is divided into the following six steps:

(1) Physical resources distributed around the world are packaged by resource creators according to standard specifications to form resource packages.

(2) The resource package is uploaded to the platform through the registration interface provided by the resource sharing platform.

(3) The resource sharing platform carries out standardized testing on the resources, extracts metadata information through the testing, and stores the metadata information in the registration information database.

(4) The resource sharing platform stores the resource package in the standard resource package database.

(5) The resource sharing platform obtains the resource metadata information from the registration information database and publishes it on the platform for users to use.

(6) The user gets the detailed information of the resource, which is obtained from the resource package by the platform.

2.3.2 Resource sharing

According to the above analysis, combined with the experience of the resource sharing project, it can be summarized that the realization of resource sharing needs to go through three stages: resource production, resource registration, resource release and use, and the specific process of resource sharing is shown in Figure 6.

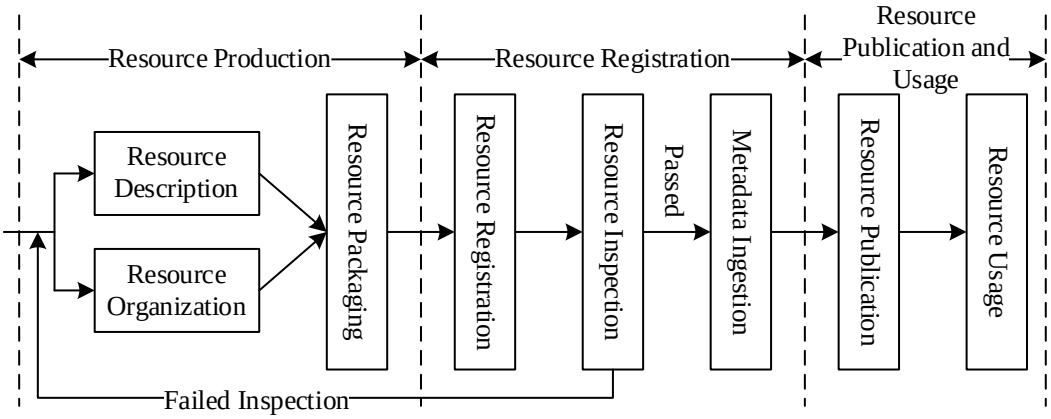

Figure 6: The process of resource sharing

(1) Resource production

To complete the resource production needs to complete three tasks: resource description, resource organization, resource packaging. Meanwhile the resource production process is divided into four steps:

1) Analyze the resource structure. Use the tree structure analysis method to determine the values of nodes, child nodes, leaf nodes and leaf nodes. Take a course as an example to analyze its structure.

2) Prepare low-granularity resources. Low-granularity resources refer to nodes with actual values, i.e. leaf nodes. For a course, it is the specific learning content at the end. Preparing these resources means collecting them and ensuring that the specific content of these resources is available at the end.

3) Describe the resources. The resources are described according to the XML binding specification, including the metadata information of the resources, the organization of the resources, the metadata information of the low-granularity resources and the access address of the low-granularity resources.

4) Resource Packaging. Ensure that the physical resources in the resource description file refers to the location, the description file and the relevant format definition file in the root directory, the file will be compressed into a resource package, resource production is complete.

(2) Resource registration

The process of resource registration can be described as follows: the user uploads the resource package to register the resource, the system detects the legitimacy of the resource, and if it is legitimate, extracts the metadata information of the resource, and enters the metadata information into the database, and uploads the resource package to the file server or Web server and other servers capable of storing files.

(3) Resource Release and Use

The following two steps are required to complete the process of resource release and use: 1) the resource sharing platform obtains the resource metadata information from the registration information database; 2) the platform obtains the resources from the resource package.

3 Digital protection technology validation and performance analysis

The historical photo restoration, site 3D reconstruction and resource management strategies proposed in Chapter 2 constitute a complete technical chain for the digital protection of red cultural resources. This chapter begins with the restoration of historical photos, analyzing the superiority of VAE algorithm from objective indicators to subjective feelings. Then it goes deeper to the three-dimensional spatial accurate reconstruction, and finally completes the comprehensive review of the comprehensive effectiveness of the whole technical system.

3.1 Research on VAE-based restoration algorithms for historical photos

The image restoration performance of the VAE algorithm is first validated and compared with multiple restoration methods. A comprehensive assessment is made in terms of both objective metrics and subjective restoration quality.

Two datasets are used for the experiments. One is based on the DIV2K composite dataset, which contains 6237 images of various low-quality generalized images; the other is the RealPhoto dataset, which is 3822 old historical photos collected in real red historical and cultural scenes.

The comparison algorithms include five algorithms, OWA, DIP, EC, DFDNet, and TDT.

3.1.1 Analysis of objective indicators

The objective evaluation mainly compares the evaluation metrics of PSNR (image signal-to-noise ratio) and SSIM (structural similarity). Each model network training scale $s \in \{2,3,4\}$, the objective performance of each model under the two datasets is shown in Table 1.

Table 1: The objective performance of each model on the two datasets

Scale	Model	DIV2K		RealPhoto	
		PSNR	SSIM	PSNR	SSIM
2	OWA	31.11	0.764	32.25	0.795
	DIP	31.83	0.783	32.82	0.807
	EC	32.46	0.809	33.11	0.855
	DFDNet	34.97	0.838	35.63	0.854
	TDT	36.07	0.855	36.69	0.859
	VAE	38.36	0.888	38.98	0.912
3	OWA	28.92	0.727	29.53	0.756
	DIP	29.94	0.754	30.85	0.801
	EC	30.09	0.796	30.67	0.821
	DFDNet	32.96	0.806	33.57	0.832
	TDT	34.83	0.821	35.87	0.850
	VAE	35.52	0.850	36.28	0.896
4	OWA	26.58	0.686	27.20	0.718
	DIP	27.16	0.709	28.25	0.737
	EC	27.26	0.758	28.36	0.783
	DFDNet	30.52	0.771	31.46	0.797
	TDT	31.99	0.789	32.99	0.809
	VAE	33.19	0.805	34.11	0.838

Both on the DIV2K generalized dataset containing various classes of old photos and on the RealPhoto old photos based on red historical scenes, the VAE algorithm in this paper achieves the highest PSNR and SSIM values at all scales, implying that the VAE model performs the best in terms of pixel restoration and overall structural fidelity. The scores of all models decreased with increasing restoration scales, which is due to the fact that the higher the restoration magnification, the more difficult it is.

Meanwhile, the advantage of VAE model is more obvious on the RealPhoto dataset than on the generalized DIV2K dataset, and the SSIM of VAE on RealPhoto is as high as 0.912 at the s2 scale, which is 6.17% higher than that of the second-place TDT model, which is 0.859. It shows that the self-splitting autoencoder VAE, based on its human-oriented content characteristics, is set up in the model to support multiple degradation restoration mechanisms as well as face detection and face enhancement restoration details, thus demonstrating stronger adaptability and restoration potentials when confronted with the real red cultural and historical background photographs.

3.1.2 Comparison of subjective repairs

A user research survey was used for subjective restoration quality evaluation, 10 old photos were randomly selected for testing in the DIV2K and RealPhoto datasets respectively, and 50 users were invited to rank the results of the six models after restoration, and the results are shown in Table 2. Meanwhile, in order to show the distribution of each model to the top three rankings more clearly, the mulberry plots of model-ranking on the two datasets are also drawn as shown in Fig. 7 and Fig. 8.

Figure 2: Ranking of subjective repair quality evaluation results of 6 models

	DIV2K			RealPhoto		
	TOP1	TOP2	TOP3	TOP1	TOP2	TOP3
OWA	0	1.23	10.65	0	0	1.08
DIP	0	3.39	20.31	0	2.34	3.39
EC	3.04	13.47	32.31	2.26	6.89	14.31
DFDNet	5.17	20.23	30.92	4.11	15.34	50.28
TDT	8.83	50.45	27.32	5.24	67.09	27.67
VAE	82.96	11.23	5.81	88.39	8.34	3.27

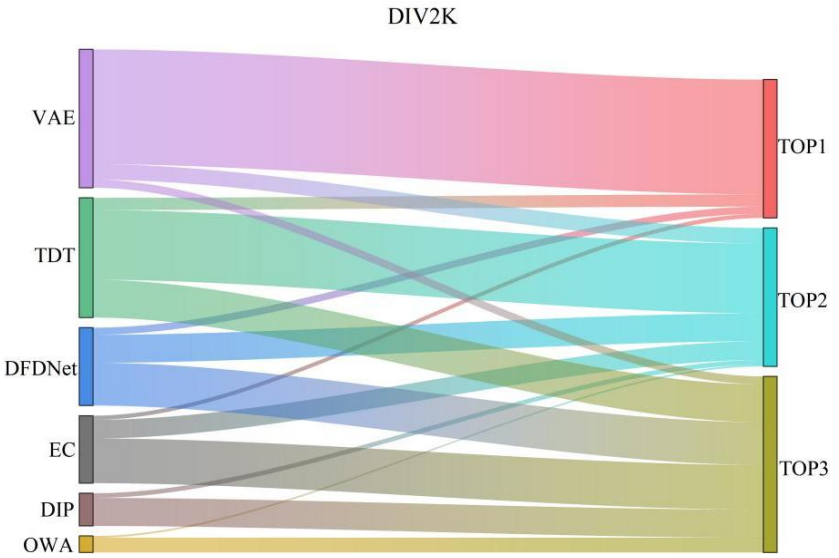

Figure 7: Ranking of models on the DIV2K dataset - Screenshot of the graph

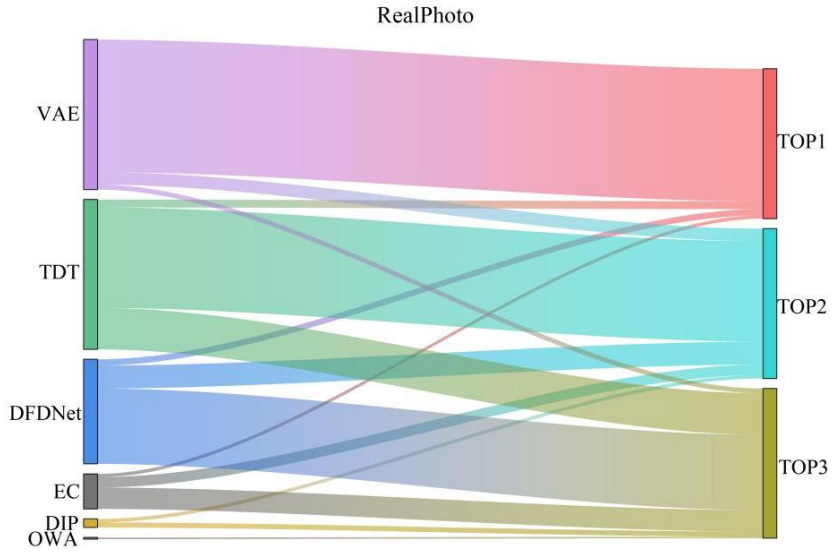

Figure 8: Ranking of models on the RealPhoto dataset - Screenshot of the graph

It can be seen that the 50 users are very satisfied with the quality of the restored photos under the VAE model, and under the DIV2K dataset, an average of 82.96% of the users think that the quality of its restoration is ranked first, and it can be found that all the photos restored by the VAE model are all flowed into the top three rankings, which intuitively proves that its

restoration effect is excellent in the level of human visual perception. For the RealPhoto dataset of old photos of real red historical scenes, the VAE model shows its advantages even more, with 88.39% of the users rating its restoration results as the first place, which is undoubtedly a monopoly.

Comparing to other models, like the TDT algorithm, there is only a 5.24% probability of flowing to the TOP1 on the RealPhoto dataset, but 67.09% flowed to the second place, i.e., users generally think that the TDT algorithm model ranks the second in terms of quality of restored photos, only after the VAE model. Similarly, more than half of the users considered the DFDNet model to be the third most effective in restoration. The other models attributed to the ranking slot did not achieve more than 80% absolute agreement like the VAE model, which side by side sets out that the photos restored based on the variational autoencoder bring users a far more comfortable feeling than other methods.

3.2 Integration and validation of techniques from point cloud simplification to mesh generation

After completing the validation of the performance of 2D historical photo restoration based on the VAE model, we now turn to the research exploration of algorithms oriented towards 3D point cloud data of site scenes. The effectiveness of the limited normal precision simplification algorithm in maintaining key features is verified, and the performance advantages of the partitioning algorithm in item structure reconstruction are comparatively analyzed.

3.2.1 Accuracy statistics of multi-source data fusion results

Firstly, the accuracy statistics of the multi-source data based on the simplified method of limited normal accuracy are carried out. The feature points of the external pointing check are selected from the 3D point cloud model entity after data fusion to obtain the coordinate information. Taking a historical building as an example, the actual puncturing results and 3D point cloud model results obtained are shown in Table 3.

Table 3: Actual mapping results and three-dimensional point cloud model results

P	Actual implementation results/m			3D point cloud model results/m			△S	△H
	X	Y	H	X	Y	H		
1	1353269.22	61822.63	2252.32	1353269.17	61822.44	2254.46	1.59	2.14
2	1353595.13	61830.92	2252.02	1353595.07	61830.85	2251.03	-0.83	-0.99
3	1353770.05	61813.41	2252.81	1353770.04	61813.48	2254.24	1.79	1.43
4	1353913.31	61827.24	2253.11	1353913.23	61827.26	2254.96	-1.14	1.85
5	1354117.22	61788.60	2253.84	1354117.37	61788.41	2254.96	1.23	1.12
6	1354359.51	61755.96	2251.47	1354359.53	61756.14	2251.06	1.23	-0.41
7	1354574.08	61830.98	2251.11	1354574.05	61831.10	2251.96	1.09	0.85
8	1354769.34	61790.44	2251.42	1354769.33	61790.38	2250.39	2.04	-1.03
9	1354875.75	61820.81	2253.72	1354875.88	61820.81	2253.04	0.85	-0.68
10	1354904.85	61752.53	2251.32	1354904.77	61752.52	2250.30	1.73	-1.02

From the 10 points listed above, it can be found that the coordinates (X, Y) of the points obtained by the 3D point cloud model, the maximum error is not more than 20cm, so that the area fluctuates between 0.83-2.04m2, and the maximum error in height is only 2.14m, and most of the point errors fluctuate around ±1m. Considering the height of the historical building itself and the complex roof structure, this level of accuracy satisfies the error requirements for point cloud data in the professional specifications.

3.2.2 Comparison of reconstruction method selection

Having verified that the model meets the point cloud accuracy requirements, we now turn to how these high quality point clouds can be used to assemble 3D models that are both realistic. This section examines the reconstruction performance of the partition-based algorithm for the interior objects of historical buildings.

The evaluation metrics CD, V-IoU, and Surface F1 are selected to test the performance of the reconstruction model under this paper's partition-based algorithm in the ShapeNet dataset.

CD is used to measure the Euclidean distance between two point clouds to evaluate the degree of similarity between two sets of point clouds.The smaller CD is, the more similar the point clouds are to each other.

V-IoU calculates the similarity of the overlapping parts between two 3D objects. It does this by calculating the ratio between the intersection volume and the concatenation volume of the two objects.

Surface F1 is a metric used to measure the accuracy of surface reconstruction of 3D objects. Based on the concept of F1, F1 is the reconciled average of precision and recall in a binary classification problem.

ShapeNet is a generalized dataset containing a large number of 3D models of objects, and the furniture, office supplies and living objects on display in the revolutionary memorial halls and historical residences are selected as the main research objects, which include the categories of tables, chairs, sofas, table lamps and other objects.

Two popular generation algorithms, the point-by-point insertion method and the triangular mesh growth method, are selected for comparison, and the reconstruction results of each object in the ShapeNet dataset are shown in Table 4.

Table 4: The reconstruction results of each item in the ShapeNet dataset

	Divide-and-conquer algorithm			Point-by-point insertion method			Triangulation network growth method		
	CD	V-IoU	F1	CD	V-IoU	F1	CD	V-IoU	F1
Table	**0.25**	**0.58**	**86.32**	0.41	0.52	82.15	0.38	0.55	83.74
Chair	**0.31**	0.51	**85.11**	0.48	**0.54**	**85.02**	0.42	0.49	82.56
Wall	**0.18**	**0.72**	**89.45**	0.29	0.65	85.33	0.35	0.63	83.91
Window	**0.22**	**0.61**	**84.27**	0.33	0.57	83.50	0.31	0.55	81.89
Sofa	**0.35**	**0.56**	**85.63**	0.52	0.49	81.24	0.47	0.51	82.77
Lamp	0.47	0.43	78.95	**0.41**	**0.48**	**80.11**	0.50	0.41	76.82
Telephone	**0.28**	**0.66**	**87.01**	0.39	0.59	83.45	0.36	0.61	84.92
Rifle	0.53	0.39	75.48	**0.49**	0.37	74.21	0.55	**0.41**	**76.80**
Average	**0.32**	**0.56**	**83.91**	0.42	0.53	82.01	0.42	0.52	81.68

It can be concluded that the partitioning algorithm achieves mostly excellent results in each evaluation metric, with the optimal number of CDs being 6, the optimal number of V-IoUs being 5, and the optimal number of Surface F1 Socore being 7. The partitioning algorithm alone accounts for 16 out of the 24 individual optimal values for all 8 types of objects, with an optimal ratio of 66.67%. The average CD value is 0.32, which is significantly lower than the 0.42 of the point-by-point insertion method and the triangular mesh growth method.Specifically, the partition algorithm performs stably on large-size objects such as walls and sofas, and also achieves the excellent results of CD= 0.28, V-IoU =0.66, and F1= 87.01 on small objects such as telephones, which proves its strong adaptability in dealing with geometric features at different scales. In contrast, the point-by-point insertion method excels on the table lamp, an

object with complex curved surface structure, and bags the optimal values of the three metrics, while the triangular mesh growth method demonstrates a unique advantage on the rifle, an object with elongated features. The partitioning algorithm reconstructs the best results.

4 Study on the application of the Red Resource Sharing Model

Based on the "distributed storage, centralized management" resource management and sharing model constructed in Section 2.3, a series of comprehensive application performance tests are conducted in this chapter. Two resource sharing models with different management styles, namely, centralized repository model and peer-to-peer distributed model, are introduced for comparison in terms of three dimensions, namely, task processing capability, network interference resistance and practical application performance.

Based on the computational volume of the shared tasks, the red cultural resources are categorized into three task types: text, photo and video.

4.1 Model task assignment performance study

Firstly, the performance of the distributed + centralized resource management model for different task assignments is verified, which is measured by analyzing the throughput of different models during the task assignment process. Meanwhile, in order to realize the simulation of user requests under different job states, this study sets up corresponding experimental conditions during simulation experiments, i.e., Poisson job and non-Poisson job. The throughput of the models at different times under the two job modes are shown in Fig. 9 and Fig. 10, respectively.

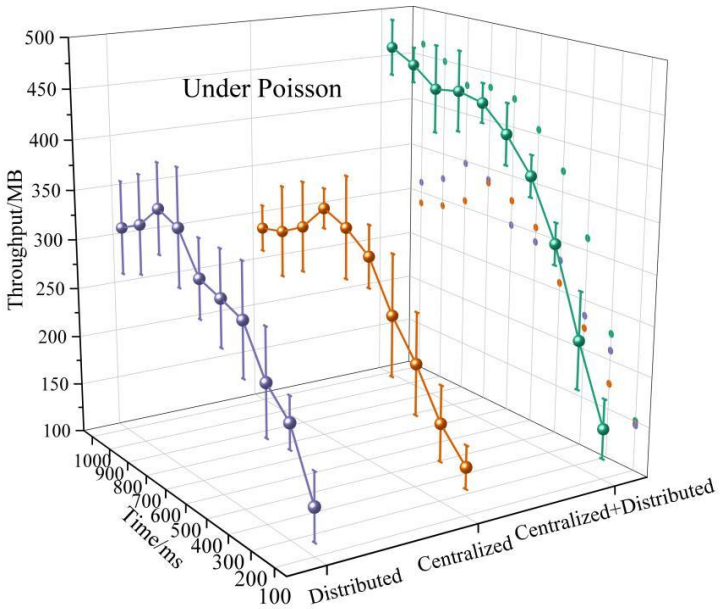

Figure 9: The throughput of the model at different times under Poisson

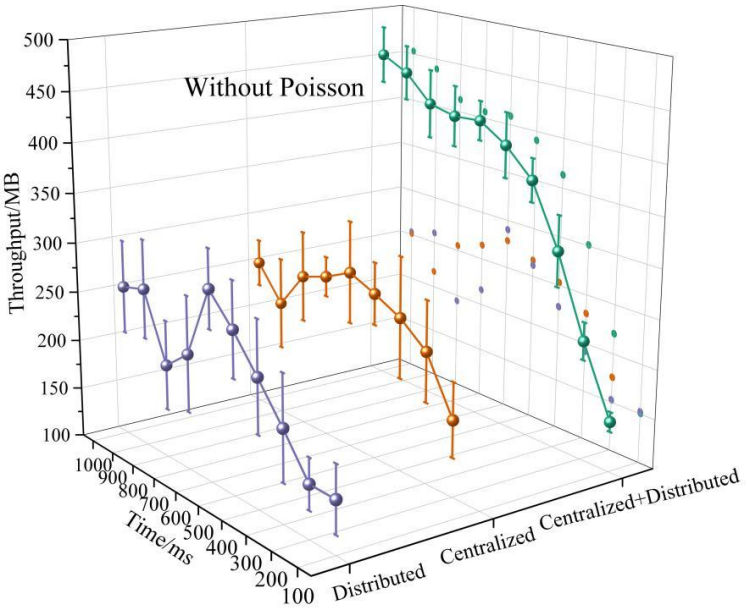

Figure 10: The throughput of the model at different times without Poisson

Under the Poisson operation condition of stable inflow, the throughput of the model in this paper is relatively high and shows a gradual upward trend, reaching a maximum of 461 MB. its data throughput is the highest in the measurement data of 0-1s at 100ms intervals, whereas in terms of the purely distributed and centralized resource management models, both of them do not have much change in the throughput after 700ms, which fluctuates between 290 and 310 MB, respectively, and They even start to decline slowly, exposing their bottlenecks in resource scheduling and stress resistance. This shows that the hybrid architecture of "distributed storage, centralized management" in this paper successfully draws the essence of both, avoiding the single-point congestion of the centralized approach and overcoming the scheduling inefficiency of the distributed approach, thus realizing efficient and reliable task allocation.

Under non-Poisson operation conditions, the throughput of this paper's model is also consistently the highest during the effective experiment time, only a slight decrease compared to the throughput under Poisson operation, which is 453.19MB at 1000ms, but both the centralized and distributed models are experiencing a drop in the breakpoints. The distributed-centralized resource management model has higher efficiency and relatively better performance in the shared task allocation process.

4.2 Link Interference Experiment

In order to analyze the anti-jamming ability of the model, this paper generates virtual requests on the basis of the above construction of virtual tasks, and sets the arrival rate of the virtual network, which is generally 4 per second, and the probability of connection between nodes is 50%. After completing the above settings, the anti-interference ability of different models is compared and analyzed in the case of link interference, and the experimental results are listed in Table 5. Among them, the number of network requests is randomly generated and not fixed. In this regard, the virtual network reception rate index is introduced to evaluate the network reception quality.

Table 5: Link interference experiments of different sharing models

	Task	Network request volume	Network acceptance volume	Reception rate	Node mapping time/ms
Centralized+ Distributed	Text	1495	1495	100%	11.13
	Photo	1609	1609	100%	17.53
	Video	748	748	100%	20.94
Centralized	Text	1544	1328	86.01%	45.23
	Photo	1317	1082	82.16%	100.81
	Video	735	425	57.82%	216.36
Distributed	Text	1663	1241	74.62%	32.02
	Photo	1128	923	81.83%	71.66
	Video	669	409	61.14%	142.17

Obviously, the network acceptance rate of this paper's "distributed storage, centralized management" model for the three types of tasks, namely, text, photo and video of red resources, reaches 100%, which means that no user request is lost in the test. And its advantage in response speed is also obvious, with node mapping times of 11.13ms, 17.53ms and 20.94ms in the three tasks, respectively.In contrast, the centralized and distributed models not only have a significant drop in the acceptance rate when dealing with the photo and video tasks, especially the acceptance rate for the video task drops to 57.82% and 61.14%, respectively, but their node response latency is also several times longer than the integrated model, up to 216.36ms. This fully proves that the model in this paper effectively circumvents network vulnerabilities through centralized scheduling, ensures stable and efficient quality of service, and provides smooth user experience even in unreliable network links.

4.3 Utility analysis

In order to prove the practicality of the red resource sharing model based on "distributed storage, centralized management", the following experiments are designed.

4.3.1 Resource-sharing efficiency

Firstly, different red resource orders of magnitude from 500 to 5000 are set, and three management style models are utilized to conduct sharing experiments on red resources, and the results of resource uploading efficiency are shown in Fig. 11.

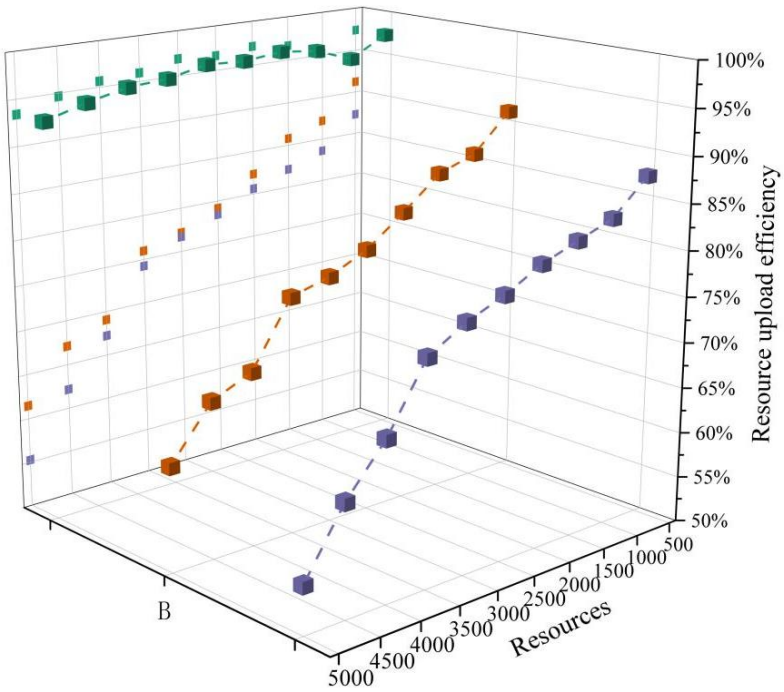

Figure 11: The results of resource upload efficiency for different sharing models

The distributed centralized model also demonstrates strong robustness in resource sharing efficiency based on the fact that its upload efficiency is always stable in the high range of 93%-97%. While the other two models based on centralized and distributed models, with the increase of the amount of resources, the efficiency declines all the way. From the figure, we can see a very obvious decline curve, when the amount of resources is 5000, the resource sharing efficiency of the centralized and distributed models has fallen to 61.47% and 55.26% respectively, almost only 60% of the efficiency of the integrated model. This eloquently proves that purely centralized or distributed architecture is difficult to cope with the growth of resource scale, and only the hybrid model can support the long-term operation of large-scale red repositories due to its optimized load distribution and metadata management, which has excellent scalability.

4.3.2 Performance of real-time resource updates

It is assumed that there are 1,000 resources that need to be updated in each of the three tasks of the studied red resources text, photo and video, and at the same time, there is a different upper limit of updating for each task category. Using the above three models to share the red resources, the results of resource sharing are obtained as shown in Fig. 12.

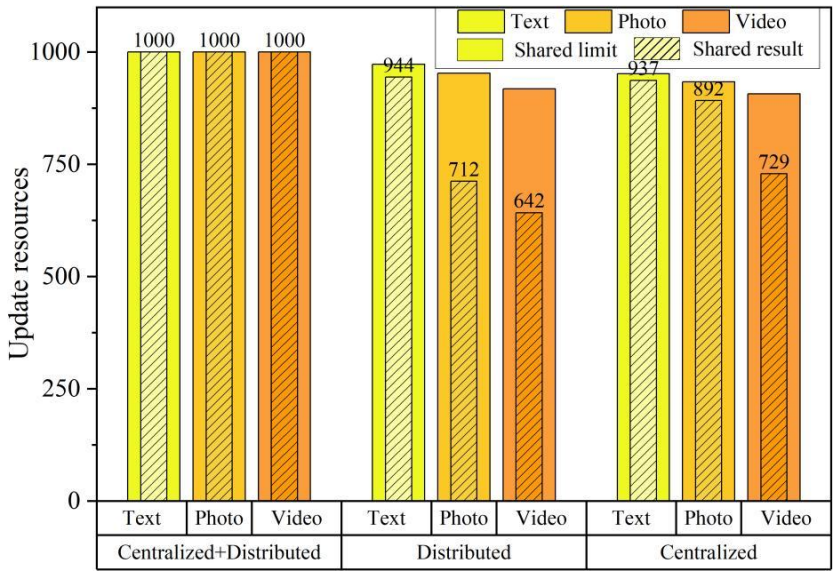

Figure 12: Different sharing models result in different resource sharing outcomes

In this paper's hybrid model, the three types of resources, text, photos, and videos of red culture, are shown as 1000/1000 under the two columns of sharing cap and sharing result. Means that it accomplishes the predefined update task 100% of the time. However, the other two models expose their architectural flaws again. They set limits at the starting point, with the centralized and distributed models sharing caps of only 973, 952 and 953, 934 for text and images, and even more caps of only 918 and 907 for video tasks. The sharing results are even more unsatisfactory, especially for the centralized model, when dealing with video update, the actual sharing result is only 642, and the update rate for the cap is only 69.93%. In contrast, the resource sharing model, which integrates centralized management and distributed storage, does a good job in ensuring the completeness and timeliness of resource updates, which is crucial for the dynamic maintenance and vigorous inheritance of red cultural resources.

5 Conclusion

The VAE-based historical photo restoration model wins the favor of more than 80% of users, and performs particularly well on the RealPhoto red cultural and historical background dataset, which still achieves a PSNR of 34.11 and a SSIM of 0.838 at the training scale s=4.

In the field of 3D reconstruction, the partitioning algorithm proves its advantage in dealing with complex historical building geometries by virtue of its overwhelming performance of capturing 16 optimums in 8 classes of objects, and its average CD value is lower than that of the comparison algorithms by about 0.1, which implies a smaller error and higher fidelity between the digital model and the real object.

In the construction of resource management model, the strategy of “distributed storage, centralized management” successfully integrates the advantages of centralized and distributed. (1) When the test time is 1000ms, the throughput of the model can still be stabilized at more than 450MB, which is about 60% higher than the traditional model; (2) In the face of network interference, the 100% request acceptance rate and the mapping latency of as low as 11ms ensure the stability and immediacy of the service; (3) When the resource scale surges from 500 to 5000, the upload efficiency of the model is as high as 93.4%, which contrasts with the centralized resource sharing model dropping to 55.26%, fully proving that its excellent scalability can continue to serve along with the growth of the red resource base.

The study builds a digital protection and inheritance path for red cultural resources from accurate restoration, to three-dimensional reproduction, to efficient resource sharing. It enables the scattered red memories to be systematically coalesced, revitalized, and transformed into digital assets for in-depth research and vivid inheritance.

Acknowledgements

The study was supported by Education Project of Industry-University Cooperation of Ministry of Education: “Innovative Teaching Reform of Aviation Literature Course in Colleges and Universities” (231102495270652); “Xi'an Aeronautical University Higher Education Teaching Reform Research Project” (Grant No. 25JXGG20010).

About the Author

Dan Wu, Doctor of Literature, Lecturer. Graduated from the Henan University in 2018. Worked in Xi’an Aeronautical University, China. Her research interests include contemporary literature and cultural communication.

References

[1] Noev, N. (2015). Approaches and Methodologies of Creating, Storing, Presentation and Protection of Digital Resources in the Field of Cultural and Historical Heritage.. Digital Presentation and Preservation of Cultural and Scientific Heritage, (Special), 19-27.

[2] Rufián Fernández, F. J., Fernández Díaz, M., Sabrine, I., Ibáñez, J. J., Claramunt-López, B., Escobar, A., & Gonzalez Zarandona, J. A. (2020). The documentation and protection of cultural heritage during emergencies. The International Archives of the Photogrammetry, Remote Sensing and Spatial Information Sciences, 44, 287-293.

[3] Zhang, S., & Jin, A. (2023). Research on the Value and Strategy of Red Culture Communication in Universities from the Perspective of the Internet. The Educational Review, USA, 7(8).

[4] Hombal, S. G., & Prasad, K. N. (2012). Digital copyright protection: Issues in the digital library environment. DESIDOC Journal of Library & Information Technology, 32(3).

[5] Meng, X., & Zhang, Z. (2025). Developing Digital Exhibition Construction of Intangible Cultural Heritage of Huizhou City Based on Virtual Technology. International Journal of Knowledge Management (IJKM), 21(1), 1-22.

[6] Qi, Y., & Zhou, Q. (2024). Digital protection and inheritance of intangible cultural heritage of clothing using image segmentation algorithm. Computer-Aided Design and Applications, 21, 159-173.

[7] Ji, C., & Xu, G. (2023). Digital development of cultural and creative industries under the security of 5G mobile and communication. Wireless Personal Communications, 1-15.

[8] Sørensen, T., & Klein, S. (2024). The Inheritance and Innovation of Red Culture Under the Background of a Sustainable Economy Based on Geographical Considerations.

Future-Journal of Cultural Studies and Technological Convergence, 1(1).

[9] Cheng, X., & Cui, Y. (2025). Does Red Culture Benefit Big Data Technology Innovation? Evidence from Chinese Cities. Current Science, 5(3), 2573-2592.

[10] LI, X., LI, H., & XIONG, J. (2020). Applications of virtual reality technology in the field of cultural heritage. Science & Technology Review, 38(22), 50-58.

[11] Todorov, T., & Lutfiu, S. (2023). Intellectual property protection of digital cultural heritage. Digit. Presentation Preserv. Cult. Sci. Heritage, 13, 263-268.

[12] Di Giulio, R., Boeri, A., Longo, D., Gianfrate, V., Boulanger, S. O., & Mariotti, C. (2021). ICTs for accessing, understanding and safeguarding cultural heritage: the experience of INCEPTION and ROCK H2020 projects. International Journal of Architectural Heritage, 15(6), 825-843.

[13] Cui, L. (2025). Research on the Protection of Intangible Cultural Heritage Based on Virtual 3D Animation Technology. International Journal of Cognitive Informatics and Natural Intelligence (IJCINI), 19(1), 1-23.

[14] Rouhani, B. (2025). From ruins to records: Digital strategies and dilemmas in cultural heritage protection. J. Art Crime, 2025, 35-51.

[15] Fang, J., Li, J., Liu, S., & Zhang, Y. (2024). Harnessing digital innovation for cultural heritage: a study on communicating West Lake folk tales through digital picture books. International Communication of Chinese Culture, 11(2), 259-279.

[16] Wu, C. H., Chao, Y. L., Xiong, J. T., & Luh, D. B. (2022). Gamification of culture: A strategy for cultural preservation and local sustainable development. Sustainability, 15(1), 650.

[17] Zhang, J., & Li, Y. (2024). Copyright protection: a key element in realizing the development potential of digital cultural and creative products in museums. Museum Management and Curatorship, 39(4), 497-517.

[18] Huang, M., & Zeng, X. (2024). Digital Protection and Innovative Development Path of Red Culture Resources Based on Distributed Machine Learning Supported by Intelligent Information. Journal of Combinatorial Mathematics and Combinatorial Computing, 120, 381-391.

[19] Huang, A. (2023, August). Research on Digital Protection Education of Red Culture Based on Big Data Technology. In 2023 International Conference on Data Science & Informatics (ICDSI) (pp. 194-198). IEEE.

[20] Tan, L., & Liang, R. (2023, July). Research on the Design of Red Cultural and Creative Products Based on Digitalization. In International Conference on Human-Computer Interaction (pp. 162-171). Cham: Springer Nature Switzerland.

[21] Jiang, H., & Yan, J. (2024). Research on Digital Protection of Red Culture in Jiangxi Province Based on Landscape Gene Theory. Academic Journal of Humanities & Social Sciences, 7(10), 64-68.

[22] XiaYan, W., LiQing, H., MingZhu, L., & Lei, Y. (2020, December). Application and Innovation of Digital Technology in the Design of Red Cultural and Creative Products:—Take Zhenjiang Maoshan New Fourth Army Red Culture as an example. In 2020 International Conference on Innovation Design and Digital Technology (ICIDDT) (pp. 487-490). IEEE.

[23] Kang, Y., & Liang, Z. (2020, December). The digital preservation and presentation of red cultural heritages in Ganjiang River Basin, China. In 2020 International Symposium on Advances in Informatics, Electronics and Education (ISAIEE) (pp. 6-14). IEEE.

[24] Miao, F., & Zhang, N. (2024). Digitization, Preservation, and Dance Narrative Exploration of Red Music Cultural Heritage in Hebei Province: A Multidisciplinary Approach. International Journal of Social Sciences and Public Administration, 2(2), 211-221.

[25] Zhang, M., Cao, Y., & Ma, Z. (2024, December). The Application of Digital Media Technology in the Innovation of Red Culture. In 4th International Conference on New Media Development and Modernized Education (NMDME 2024) (pp. 244-255). Atlantis Press.

[26] Wang, L., Zhang, X., & Cao, W. (2025, August). The innovative design and application of virtual reality technology in the Red Culture Exhibition Hall. In 5th International Conference on Internet of Things and Smart City (IoTSC 2025) (Vol. 13739, pp. 205-211). SPIE.

[27] BAO, Y., LV, Y., & WANG, J. (2024). STUDY ON THE PATH OF INNOVATIVE TRANSFORMATION OF YAN'AN RED CULTURAL RESOURCES EMPOWERED BY DIGITIZATION. FRONTIERS, 4(12), 329-337.

[28] Liying, F., Weng, N. G., Liyao, M., Maozheng[1], F., & Xiaoping[1], Q. (2022, March). Research on the Application of Augmented Reality Technology in the Transformation and Development of Cultural and Creative. In Intelligent Technologies for Interactive Entertainment: 13th EAI International Conference, INTETAIN 2021, Virtual Event, December 3-4, 2021, Proceedings (Vol. 429, p. 295). Springer Nature.

[29] Huang, Z., Zhan, Z., Gao, H., & An, W. (2024, May). Research on the Mechanism of Cultural Identity Impact under the Integration of Red Tourism and Cultural Tourism Empowered by Digital Technology. In Proceedings of the 2024 International Conference on Digital Society and Artificial Intelligence (pp. 451-456).

[30] Zhuang, S. (2023). Research on the Design of Changting Red Culture Apps Based on Emotional Design. INNOVATION, 11, 142-147.

[31] Xie, B. (2024). Digital protection and dissemination of red cultural resources based on the Internet of Things and big data. Journal of Computational Methods in Sciences and Engineering, 14727978251367169.